Direct measurements of spin relaxation times of electrons in tunnel-coupled Ge/Si quantum dot arrays

A. F. Zinovieva,* A. V. Dvurechenskii, N. P. Stepina, A. I. Nikiforov, and A. S. Lyubin
Institute of Semiconductor Physics, SB RAS, 630090 Novosibirsk, Russia

L. V. Kulik
Institute of Chemical Kinetics and Combustion, SB RAS, 630090 Novosibirsk, Russia
(Received 3 April 2009; revised manuscript received 22 January 2010; published 12 March 2010)

Electron paramagnetic resonance and spin-echo methods are used to probe the spin dynamics in Ge/Si heterostructures with quantum dots. A spin coherence time of up to 20 μs is obtained for electrons confined in strain-induced Si potential wells near the apices of Ge quantum dots. The measurements of spin echo confirm the model of spin relaxation through the spin precession in the effective magnetic field lying in the plane of a quantum dot array. Existence of two electron groups with different spin-relaxation times is suggested to explain a nonexponential spin-echo behavior observed in the structures under study.

DOI: 10.1103/PhysRevB.81.113303 PACS number(s): 73.21.La, 03.67.Lx, 72.25.Rb

Symmetry of nanostructure has a crucial impact on the spin dynamics. The spin-orbit (SO) coupling in asymmetrical quantum-well structures gives the possibility to manipulate the spin of electrons[1,2] but at the same time it serves as main source of spin relaxation. The extensive continuous wave (cw) electron paramagnetic resonance (EPR) experiments[3] and direct spin-coherence measurements[4] of quantum-well (QW) structures have shown that the longitudinal spin-relaxation time and the coherence time of two-dimensional (2D) electrons are controlled by the effective in-plane fluctuating magnetic field[5] whose origin is the SO interaction. This effective magnetic field $\mathbf{H}_{\text{eff}}$ describes the spin splitting induced by inversion asymmetry of the system and depends on the electron wave vector $\mathbf{k}$, $\mathbf{H}_{\text{eff}}=\alpha(\mathbf{k}\times\mathbf{e}_z)/g\mu_B$ (Refs. 3–5). Here, g is the electron g factor, μ_B is the Bohr magneton, and $\mathbf{e_z}$ is the unit vector in the growth direction of QW structure. The spin of mobile electron rotates around this intrinsic magnetic field and $\mathbf{k}$ scattering provokes a spin dephasing due to random fluctuations of the effective magnetic field. The confinement of electrons in all three dimensions switches off this efficient spin-relaxation mechanism due to vanishing of $\langle\mathbf{k}\rangle$ for localized state. Therefore, the electron localization in a quantum dot (QD) is one of promising ways to preserve a spin orientation. The silicon-based QDs are currently considered as one of the best candidates for solid-state implementation of spintronics and quantum-computation schemes because of the long spin lifetime in silicon, originating from weak SO coupling and extremely small concentration of nuclear spins in Si (a natural abundance of isotope ^{29}Si is less than 5%).

In the previous work[6] we made the attempts to localize the electrons in all three dimensions in Si and to measure their spin-relaxation time. For this purpose Ge nanoclusters were embedded into the Si matrix using the molecular-beam epitaxy (MBE) in Stranski-Krastanow growth mode.[7] The electrons in this system are localized in Si surrounding the Ge QDs due to misfit strain. To enlarge the electron-binding energy, the multilayer Ge/Si structure with vertical stacking of Ge QDs was formed. An accumulation of the strain from different QD layers provides the increase in potential well depth for electrons. As a result, the creation of fourfold stacked Ge/Si QDs structure allowed us to enlarge the binding energy of electrons up to ~60 meV (Ref. 8) that is larger than the binding energy of shallow donors in Si (~40 meV). A depletion of donors at low temperatures and localization of electrons at the apices of Ge dots were proved by EPR measurements in cw mode. We observed a special EPR signal with anisotropic line width. An analysis of the obtained g-tensor values confirmed the relation of this signal to electrons localized in strain-induced potential wells in the vicinity of Ge QDs. For explanation of the orientation behavior of EPR line width we proposed the model of anisotropic spin relaxation due to the interaction of electron spin with the effective magnetic field lying in the plane of the QD array. The cause of this effective field in the QD system is the same as in 2D QW structures [a structure-inversion asymmetry (SIA) of electron potential wells]. However there are some peculiarities for localized states in the QD system. The fact is that the localization of carrier in all three dimensions leads to the uncertainty of electron momentum Δk_x, Δk_y, Δk_z. This uncertainty provides the appearance of the effective magnetic field $\mathbf{H}_{\text{eff}}=\alpha_{\text{QD}}(\Delta\mathbf{k}_{x,y}\times\mathbf{e}_z)/g\mu_B$ with a random in-plane direction (Fig. 1). Obviously, the average value of this field equals to zero for the localized state in QD.

However, during tunneling between coupled QDs the preferential tunneling direction $\mathbf{n}$ appears, which defines the direction of the effective magnetic field: $\mathbf{H}_{\text{eff}}=\alpha_{\text{QD}}\Delta k_n(\mathbf{n}\times\mathbf{e}_z)/g\mu_B$. Every tunneling event is accompanied by the small spin rotation in the effective magnetic field that provokes the spin flip after series of random tunneling events.[9] The tunneling (hopping) direction $\mathbf{n}$ in QD system serves as analog of the electron momentum direction $\mathbf{k}/k$ in 2D system. When the external magnetic field is oriented perpendicularly to the QD plane, the model implies a special relation between values of T_2 (a coherence time) and T_1 (a spin-population-relaxation time), $T_2=2\,T_1$. This is a consequence of in-plane arrangement of fluctuating effective magnetic fields. The longitudinal relaxation arises entirely from H_x and H_y components, $1/T_1\sim H_x^2+H_y^2$ (Ref. 10). While the transverse relaxation is defined by the average squared compo-

 ©2010 The American Physical Society

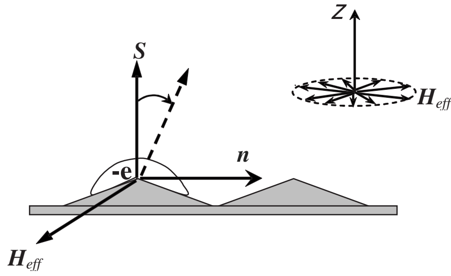

FIG. 1. Scheme of a tunneling process and a spin rotation around the effective magnetic field. Here n is the tunneling direction, S is the electron spin, and H_{eff} is the effective magnetic field, arising during tunneling between QDs. The right-hand picture shows the uncertainty of the effective magnetic field for localized state in QD (Ref. 9) and Z is the growth direction of the QD structure.

nent of the field that is transverse to a spin lying in plane of QD array, $1/T_2 \sim 1/2(H_x^2+H_y^2)$.

The experimental observation of the relation $T_2=2\ T_1$ provides a strong evidence of proposed model of anisotropic spin relaxation. However, in the case of inhomogeneous broadening of the EPR line, which is typical for self-assembled QD structures, a conventional cw EPR experiment is not sufficient for determination of spin-relaxation times and the pulse mode measurements are more powerful. In the present work the spin-echo method is used for direct measurements of T_2 and T_1 values in the multilayered Ge/Si QD system and the relation between them is compared with prediction of the model.

Samples were grown by MBE on n-Si(001) substrates with a resistivity of 1000 Ω cm. During growth procedure a fourfold stack of Ge islands was inserted into the 0.6 μm epitaxial n-Si layer (Sb concentration 4×10^{16} cm^{-3}) at the distance of 0.3 μm from the substrate (Fig. 2). In order to reduce distortion of the electron-confining potential by the potential of ionized impurities, a 10-nm-thick undoped Si spacer was introduced between the topmost Ge layer and the n-type Si cover layer. The first and the second Ge layers as well as the third and the fourth ones are separated by 3-nm-thick Si spacers while the distance between the second and the third Ge layers is 5 nm. The Ge QD's formation was controlled by reflection high-energy electron diffraction. After growth, the test samples were analyzed by transmission

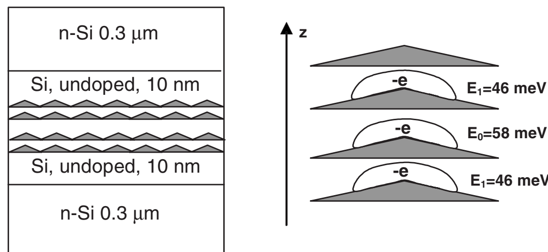

FIG. 2. Structure of the sample and scheme of electron localization. The energies of the ground-electron state (in central Si spacer) and the first two excited-electron states (in top and bottom Si spacers) are given according to results of numerical calculations (Ref. 8).

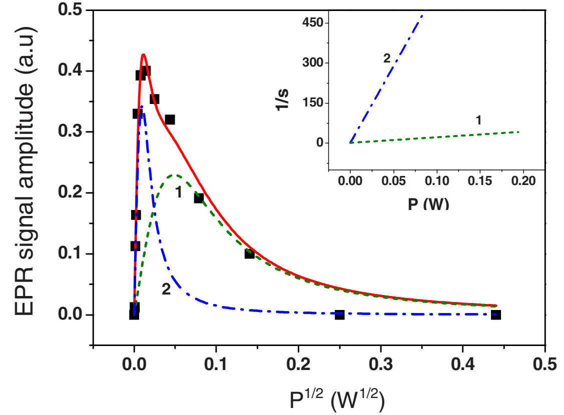

FIG. 3. (Color online) Saturation curve of microwave power P absorption (symbols ■ are experimental data). Solid line is a superposition of two theoretical saturation curves (dashed and dashed-dot lines) either of them corresponds to a Lorenz EPR line. Inset shows the saturation parameter s behavior for both Lorenz lines, $1/s=1+1/4\gamma^2H_1{}^2T_1T_2$, where H_1 is microwave field and γ is gyromagnetic ratio (Ref. 12).

electron microscopy. It was shown that the average lateral size of Ge nanoclusters is 20–25 nm and the height is 1.5 nm, the density of QDs is $n \sim 10^{11}$ cm^{-2}.

Measurements were performed with a Bruker Elexsys 580 X-band EPR spectrometer using a dielectric cavity Bruker ER-4118 X-MD-5. The samples were glued on a quartz holder and the entire cavity and sample were maintained at low temperature with a helium flow cryostat (Oxford CF935). To avoid the needless EPR signal from dangling bonds ($g=2.0055$) the passivation with atomic hydrogen was done before measurements. The spin-echo measurements were carried out at temperature 5 K in resonance magnetic field $H=3455$ G (can be slightly varied ±5 G in dependence on resonance conditions), $\mathbf{H}\|Z$, where Z is the [001] growth direction of the structure. To establish the origin of the EPR line broadening and estimate the approximate values of T_1 and T_2, a preliminary study of the saturation of microwave power absorption in cw mode was performed. A two-pulse Hahn echo experiment ($\pi/2-\tau-\pi-\tau-$echo) was used to measure T_2 (a detailed explanation can be found in Ref. 11). In order to observe a longitudinal spin relaxation (corresponding time T_1), a different pulse sequence is applied ($\pi-\tau-\pi/2-T-\pi-T-$echo). The first π pulse rotates the magnetization opposite to its thermal equilibrium orientation, where the interaction with the environment causes the spins to relax back to initial orientation parallel to $\mathbf{H}$. After time τ, a $\pi/2$ pulse followed by another π pulse is used to observe a Hahn echo. In the first and second type of experiments, the durations of $\pi/2$ and π pulses were 60 and 120 ns, respectively; the interpulse time in the second experiment was kept $T=200$ ns.

Figure 3 demonstrates the dependence of EPR signal amplitude on microwave power measured in cw mode. One can see a saturation curve with a well-pronounced peak and following decay at higher power levels. The observed behavior is specific for homogeneously broadened EPR line;[12] however, there is apparent non-Lorentzian behavior. The experi-

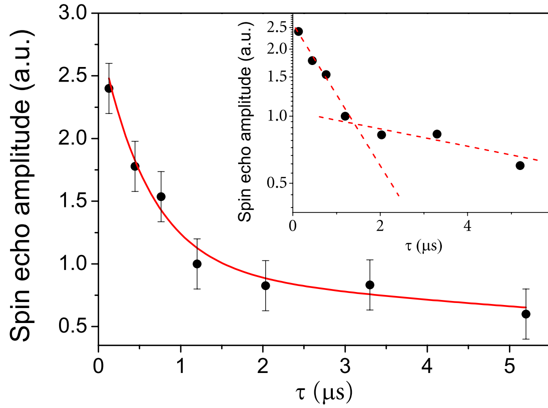

FIG. 4. (Color online) Amplitude of spin-echo signal versus delay time τ (symbols ● are experimental data, solid line is a superposition of two exponential functions). Inset shows the spin-echo decay in semilogarithmic scale. Corresponding microwave pulse sequence is $\pi/2-\tau-\pi-\tau-$echo.

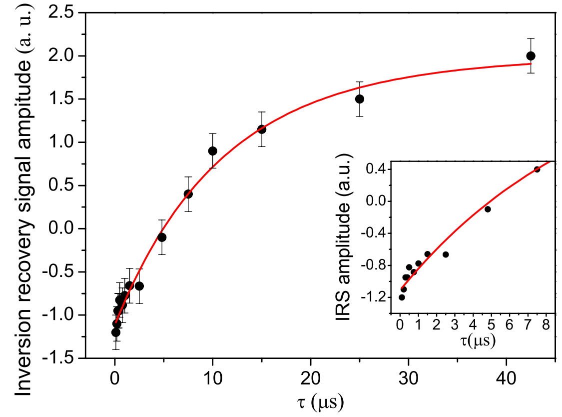

FIG. 5. (Color online) Amplitude of inversion-recovery signal versus interpulse delay τ (symbols ● are experimental data). Inset shows the early stage of inversion recovery. Corresponding microwave pulse sequence is $\pi-\tau-\pi/2-T-\pi-T-$echo.

mental saturation curve is described by a superposition of two saturation curves either of them corresponds to a Lorentz line. It means that there are two groups of electrons with different spin-relaxation times contributing to the observed EPR line. Inset shows the behavior of the saturation parameter s for both Lorenz lines. From the equation $1/s=1+1/4\gamma^2 H_1{}^2 T_1 T_2$, where H_1 is microwave field, γ is gyromagnetic ratio,[12] we can determine the products of transverse and longitudinal spin-relaxation times for both lines. For the first line this product (T_1T_2) is about 10^{-12} s^2, for the second line $T_1T_2\sim 10^{-10}$ s^2.

While the saturation experiments give the product T_1T_2 only, the measurements of spin echo allow us to obtain the exact values of both relaxation times independently. In the Fig. 4 the spin-echo decay measured in two-pulse Hahn echo experiment is shown. Inset to Fig. 4 demonstrates that the spin-echo behavior can be described by a superposition of two exponentially decaying functions

$$M(t) = M_{x,y}^{(1)} \exp(-2\tau/T_2^{(1)}) + M_{x,y}^{(2)} \exp(-2\tau/T_2^{(2)}),$$

where $M(0)=M_{x,y}^{(1)}+M_{x,y}^{(2)}$ is the lateral (in QD plane) magnetization after $\pi/2$ pulse. Decay parameters $T_2^{(1)}$ and $T_2^{(2)}$, obtained by fitting the experimental data, amounts to $T_2^{(1)}\approx 0.9$ μs and $T_2^{(2)}\approx 20$ μs.

The analysis of an inversion signal recovery, measured in three-pulse echo experiments, shows a nonexponential behavior (Fig. 5) that can be described by the superposition of two functions

$$M(t) = M_{0z} - M_z^{(1)} \exp(-\tau/T_1^{(1)}) - M_z^{(2)} \exp(-\tau/T_1^{(2)}),$$

where M_{0z} is the equilibrium magnetization, $M_{0z}=M_{0z}^{(1)}+M_{0z}^{(2)}$, $M_z^{(1,2)}=M_{0z}^{(1,2)}-M_z^{(1,2)}(0)$, and $M_z(0)=M_z^1(0)+M_z^2(0)$ is the magnetization just after applying of an inverting π pulse. The experimental curve consists of two pieces with different recovery rates. At the beginning the sample magnetization recovers very fast. After some time the part of spins is returned to an equilibrium state and the recovery rate becomes much slower. The relaxation times $T_1^{(1,2)}$ for both pieces of curve can be extracted from the last equation for $M(t)$. The characteristic time obtained by this fitting for the first rapid stage of recovery is about $T_1^{(1)}\approx 400$ ns while for the second stage it is $T_1^{(2)}\approx 10$ μs. All values of spin-relaxation times were determined with the error $\pm 20\%$.

Thus, the spin-echo measurements confirm the finding of saturation experiments that two groups of carriers with different T_2 and T_1 define the spin dynamics in the structure under investigation. In both groups of carriers the special relation between T_2 and T_1, $T_2\approx 2T_1$, is observed. The unusual relation $T_2>T_1$ confirms that the spin relaxation is caused by the interaction with the effective magnetic field arising due to the SIA. However, to make a final conclusion about mechanism of spin relaxation we should demonstrate that the emission/absorption of phonons has negligible contribution to the spin relaxation. A comparison of SIA mechanism and phonon mechanism of spin relaxation, made as in our previous paper,[13] shows several orders of magnitude difference between corresponding spin-relaxation times. We find that the phonon-induced spin-relaxation time for ground-state electrons is about 50 s (at temperature 5 K and external magnetic field $H=3455$ G). Such long time is a consequence of small SO interaction in Si and special electronic structure of fourfold Ge QD stack[8]).

Let us discuss the possible reasons of existence of two groups of electrons with different spin-relaxation times. The basis of proposed mechanism of spin relaxation is nonzero probability of tunneling transitions between QDs. Every electron hopping from one dot to another causes a small rotation of the spin. Eventually the spin relaxes after a large number of random tunneling transitions, which leads to averaging of the spin-relaxation time. As a result, a single group of electrons should be detected. We propose the following explanation of the appearance of the second group of electron with another relaxation rate. At first, to avoid the averaging between two groups of electrons, they should be spatially separated. Indeed, in fourfold stacked QD structure, electrons can be localized in different Si spacers. According to the numerical calculations, using the effective-mass approximation,[8] the ground state of the electron (E_0

$=58$ meV) is formed in the central Si spacer while the first and second excited states ($E_1=E_2=46$ meV) are formed in the upper and lower Si spacers. Size distribution of QDs results in the energy level spread (≈ 10 meV), which is comparable with the energy difference between ground and excited states. As a result, electrons can be located in the ground state as well as in the first two excited states, and, hence, in different Si spacers. The scheme of electron localization in the fourfold stacked QD structure is shown in the right panel of Fig. 2. The vertical electron transitions between Si spacers are suppressed by Ge barriers, which prevent the averaging between electron groups.

Different spin-relaxation times can be resulted from different tunneling probabilities of electrons in the central and top (bottom) Si spacers. It is obvious that the higher tunneling probability the faster electrons lose the spin orientation. The tunneling probability depends on the height of potential barrier between QDs. These barriers arise due to in-plane strain modulation induced by QDs in Si layers. Strain modifies the conduction band edge and determines the height of the barrier between QDs through deformation potential.[8] The numerical calculations of the strain distribution in fourfold QD stack, using a valence-force-field model with a Keating interatomic potential (model parameters were taken the same as in Ref. 8), shows that the barrier height is approximately 10 meV higher for the top and bottom Si spacers as compared with the central one. Such a difference leads to one order of magnitude larger tunneling probability in the central Si layer and shorter time of spin relaxation in the corresponding electron group. According to theoretical estimation, using equations from Ref. 14, the rate of hopping transitions between QDs in the central Si layer is 10^{10} s^{-1} (at temperature 5 K) while in the adjacent Si layers it is 10^9 s^{-1} that is in agreement with the experimental values of spin-relaxation times.

In conclusion, our results of spin-echo measurements confirm that the interaction with the effective magnetic field is the main source of the spin decoherence in a tunnel-coupled QD system with structure-inversion asymmetry. Two different sets for both longitudinal and transverse spin-relaxation times were obtained in experiments on four-layered QD structure. The result was interpreted as an effect of different probability of electron hopping between strain-induced localized states near Ge QDs in Si spacers with different width.

We thank A. V. Nenashev and A. A. Bloshkin who generously provided us with calculations of the strain and energy spectrum of localized electrons. This work was supported by RFBR (Grants No. 08-02-00121 and No. 09-02-90480).

*aigul@isp.nsc.ru

[1] S. Datta and B. Das, Appl. Phys. Lett. **56**, 665 (1990).
[2] J. Schliemann, J. C. Egues, and D. Loss, Phys. Rev. Lett. **90**, 146801 (2003).
[3] Z. Wilamowski, W. Jantsch, H. Malissa, and U. Rössler, Phys. Rev. B **66**, 195315 (2002).
[4] A. M. Tyryshkin, S. A. Lyon, W. Jantsch, and F. Schäffler, Phys. Rev. Lett. **94**, 126802 (2005).
[5] A. Bychkov and E. I. Rashba, J. Phys. C **17**, 6039 (1984).
[6] A. F. Zinovieva, A. V. Dvurechenskii, N. P. Stepina, A. S. Deryabin, A. I. Nikiforov, R. M. Rubinger, N. A. Sobolev, J. P. Leitao, and M. C. Carmo, Phys. Rev. B **77**, 115319 (2008).
[7] I. N. Stranski and L. Krastanow, Sitzungsber. Akad. Wiss. Wien, Math.- Naturwiss. Kl., Abt. 2B **146**, 797 (1938).
[8] A. I. Yakimov, A. V. Dvurechenskii, A. I. Nikiforov, A. A. Bloshkin, A. V. Nenashev, and V. A. Volodin, Phys. Rev. B **73**, 115333 (2006).
[9] A. F. Zinovieva, A. V. Nenashev, and A. V. Dvurechenskii, Phys. Rev. B **71**, 033310 (2005).
[10] Y. Yafet, Solid State Phys. **14**, 1 (1963).
[11] A. Schweiger and G. Jeschke, *Principles of Pulse Electron Paramagnetic Resonance* (Oxford University Press, Oxford, 2001).
[12] C. P. Poole, *Electron Spin Resonance: A Comprehensive Treatise on Experimental Techniques*, 1st ed. (Wiley, New York, 1967).
[13] A. F. Zinov'eva, A. V. Nenashev, and A. V. Dvurechenskii, JETP Lett. **82**, 302 (2005); Sov. Phys. JETP **105**, 388 (2007).
[14] A. Miller and E. Abrahams, Phys. Rev. **120**, 745 (1960).